Available online at www.sciencedirect.com
ScienceDirect
Dyes and Pigments 73 (2007) 285–291
DYES and PIGMENTS
www.elsevier.com/locate/dyepig

Synthesis and properties of long conjugated organic optical limiting materials with different π-electron conjugation bridge structure

Shanyi Guang [a], Shouchun Yin [a], Hongyao Xu [a,b,*], Weiju Zhu [a], Yachen Gao [c], Yinlin Song [c]

[a] *School of Chemistry and Chemical Engineering, Anhui University, Hefei 230039, China*
[b] *The Key Laboratory of Environment Friendly Materials of Anhui Province, Anhui University, Hefei 230039, China*
[c] *Department of Physics, Harbin Institute of Technology, Harbin 150001, China*

Received 14 August 2005; received in revised form 19 October 2005; accepted 20 December 2005
Available online 28 February 2006

Abstract

Three novel organic optical materials, 4′-(*N*,*N*-dihydroxyethylamino),4-(pyridine-4-vinyl)stilbene (**8a**), *N*-((4-*N*,*N*-dihydroxyethylamino)-benzylidene)-4-(pyridine-4-vinyl)aniline (**8b**) and 4′-(*N*,*N*-dihydroxyethylamino),4-(pyridine-4-vinyl)azobenzene (**8c**), were synthesized and characterized by FT-IR, UV, ^{1}H NMR and elementary analysis. Their optical properties were evaluated by optical limiting and nonlinear optical analyses. The results show that these compounds possess good optical limiting and large nonlinear optical properties, which are attributed to the long D-π-A conjugated electron structure of molecules, and the π-electron conjugated bridge structure affects the nonlinear optical and optical limiting properties of D-π-A conjugation compounds. The compound **8a** with C=C double bond as conjugation bridge shows better optical limiting property than compounds **8b** and **8c** with C=N or N=N double bond under the same linear transmittance, while compound **8c** with N=N double bond as conjugation bridge is superior in nonlinear optical properties to compounds **8a** and **8b** with C=C or C=N double bond as conjugation bridge.

Keywords: Optical limiter; Nonlinear optics; Z-scan; Chromophore; Synthesis; Conjugated bridge

1. Introduction

Conjugated organic materials exhibiting strong nonlinear optical properties and fast response time have attracted considerable interest in recent years because of their usages in a variety of optical devices. In particular, in recent years their applicability for optical limiters has received significant attention owing to the growing needs for protection of optically sensitive devices and human eyes from laser damage in both civilian and military applications due to the fast development of modern laser technology [1,2].

To enhance the application viability of the conjugated organic NLO materials in optical limiter devices, a collective effort from physicists, chemists and material scientists is currently in progress to understand the fundamental relationship between optical limiting property and molecular structure. Most of the studies are focused on explaining that the large atomic number and the small metallic atomic size may enhance the optical limiting properties of organic metallic compounds such as phthalocyanines and porphyrins [3–9]. Some are focused on the effect of the conjugation length and the donor–acceptor strength on the optical limiting properties of organic NLO materials [10–15]. However, little attention has been paid to the effect of the different π-electron conjugation bridge structure on the optical limiting properties of organic

* Corresponding author. Tel.: +86 551 510 7342; fax: +86 551 510 8203.
E-mail address: hongyaoxu@163.com (H. Xu).

0143-7208/$ - see front matter © 2006 Elsevier Ltd. All rights reserved.
doi:10.1016/j.dyepig.2005.12.005

NLO materials. The different π-electron conjugation bridge structure would be expected to have a significant effect on the ground and excited state dipole moments and electronic transition energies of the molecular, consequently, could affect the optical property of the molecule.

In this paper, we designed and synthesized three novel D-π-A conjugated organic optical materials, namely, 4′-(*N*,*N*-dihydroxyethylamino),4-(pyridine-4-vinyl)stilbene (**8a**), *N*-((4-*N*,*N*-dihydroxyethylamino)benzylidene)-4-(pyridine-4-vinyl) aniline (**8b**) and 4′-(*N*,*N*-dihydroxyethylamino),4-(pyridine-4-vinyl)azobenzene (**8c**) (Scheme 1), which differ only from the π-electron conjugation bridge structure, measured their optical limiting and nonlinear optical properties, and investigated the effect of molecular structure on their optical limiting and nonlinear optical properties.

2. Experimental

2.1. Materials and measurements

4-Vinylpyridine was purchased from Fluka and distilled from calcium hydride under reduced pressure before use. Palladium (II) acetate, 4-bromotoluene, triphenyl phosphine, 4-bromoaniline and *N*-bromosuccinimide were purchased from Aldrich. Triethylamine, phosphorus trichloride, *N*,*N*-dimethylformamide and all solvents were purified before use. A *tert*-butoxide–*tert*-butyl alcohol solution was prepared immediately before use.

The FT-IR spectra were recorded as KBr pellets on a Nicolet 170sx spectrometer. ^{1}H NMR spectra were collected on an AVANCE/DMX-300 MHz Bruker NMR spectrometer. Elementary analyses were conducted on Vario EL-III elementary analysis apparatus. Melting points (mp) were measured on a Yanaco micro-melting point apparatus. UV–vis spectra were recorded on a Shimadzu UV-265 spectrometer using a 1 cm^2 quartz cell.

The investigation of the optical limiting properties of the samples was carried out by using a Q-switched ns/ps Nd:YAG laser system continuum with a pulse width of 8 ns at 1 Hz repetition rate and 532 nm wavelength. The experimental arrangement is similar to that in the literature [16]. The samples were housed in quartz cells with a path of 5 mm. The input laser pulses adjusted by an attenuator (Newport) were split into two beams. One was employed as reference to monitor the incident laser energy, and the other was focused onto the sample cell by using a lens with 300 mm focal length. The sample

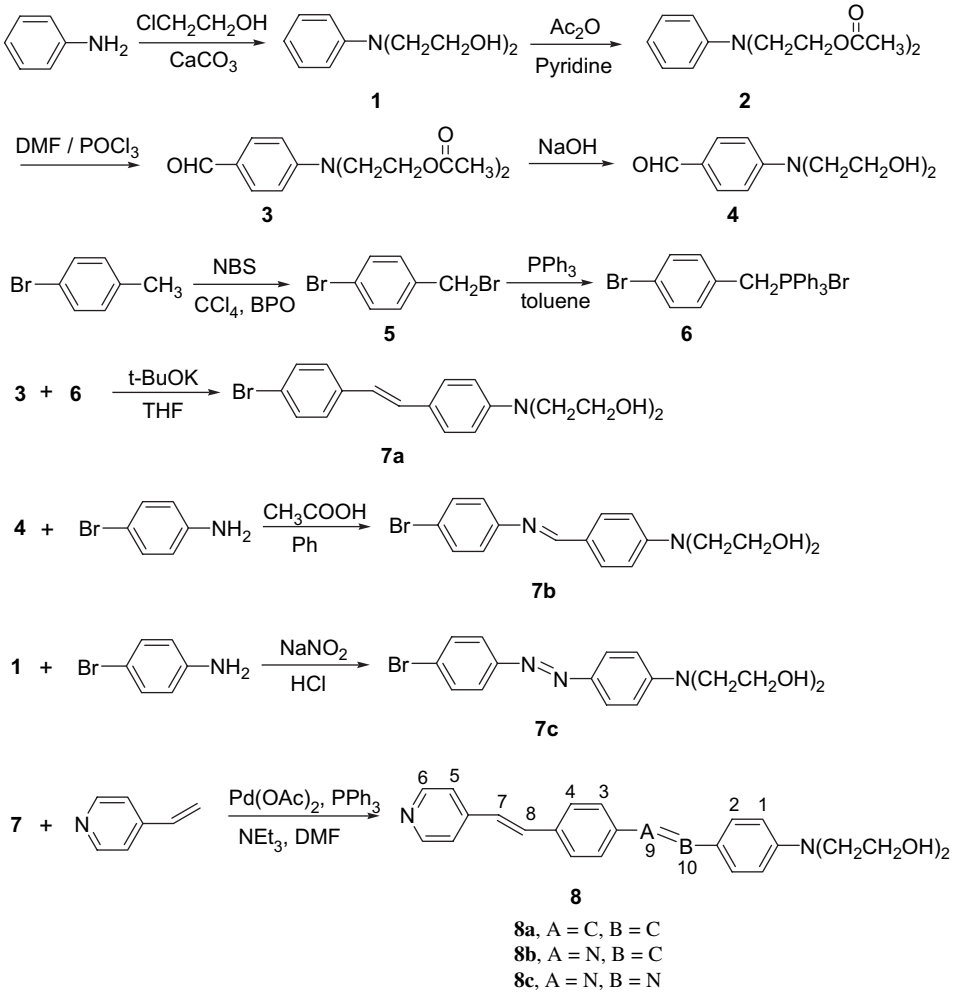

Scheme 1. Synthetic route and the serial number of hydrogen atom of benzene ring.

was positioned at the focus. The incident and transmitted laser pulses were monitored by two energy detectors, D_1 and D_2 (Rjp-735 energy probes, Laser Precision).

The nonlinear optical properties of the samples were performed by Z-scan technique with the same laser system as in the optical limiting experiment. The experiment was set up as in ref. [17]. The solution sample was contained in a 2 mm quartz cell. The incident and transmitted energies were detected simultaneously by the energy meters (Laser Precision Corporation, Rjp-735). The input energy was 100 μJ. The samples were moved along the axis of the incident beam (z direction).

2.2. Synthesis

2.2.1. N,N-Di(2-hydroxyethyl)aniline (**1**)

A mixture of 26.8 mL (0.4 mol) 2-chloroethanol, 8.9 mL (0.07 mol) aniline, 65 mL distilled water and 15 g (0.15 mol) $CaCO_3$ was refluxed for 20 h. The mixture was then filtered and the filtrate was saturated with NaCl and extracted with acetic ether. The organic layer was dried with anhydrous magnesium sulfate and concentrated by rotary evaporation. The crude product was distilled under reduced pressure to give a pale yellow viscous oil (178–184 °C/2 mmHg). Yield: 55%. FT-IR (KBr), n (cm^{-1}): 3328 (−OH), 2945, 2882 ($-CH_2$), 1597 (−Ar). ^1H NMR (300 MHz, DMSO-d_6), δ (ppm): 3.39 (4H, t, $J = 5.4$ Hz, CH_2CH_2OH), 3.52 (4H, t, CH_2CH_2OH), 4.72 (2H, s, O*H*), 6.53 (1H, dd, $J = 7.2$ Hz, 4-H), 6.66 (2H, d, $J = 8.2$ Hz, 2- and 6-H), 7.12 (2H, dd, 3- and 5-H).

2.2.2. N,N-Di(2-acetyloxy)ethyl]amino]benzene (**2**)

52 g (0.28 mol) *N*,*N*-di(2-hydroxyethyl)aniline was added to 90 g (0.88 mol) acetic anhydride and 70 g (0.88 mol) pyridine, and the resulting mixture was refluxed for 24 h. Then the reaction mixture was concentrated by rotary evaporation, washed with water and then was dried with anhydrous magnesium sulfate. The product was purified by vacuum distillation to give a yellow viscous oil of 63.8 g (86%). FT-IR (KBr), n (cm^{-1}): 1737 (C═O), 1599, 1506 (−Ar), 1231 (C−O). ^1H NMR (300 MHz, $CDCl_3$), δ (ppm): 2.11 (6H, s, CH_3), 3.59 (4H, t, $J = 6.2$ Hz, CH_2CH_2OAc), 4.23 (4H, t, CH_2CH_2OAc), 6.62 (1H, dd, $J = 7.2$ Hz, 4-H), 6.81 (2H, d, $J = 7.8$ Hz, 2- and 6-H), 7.21 (2H, dd, 3- and 5-H).

2.2.3. 4-[N,N-Di[2-(acetyloxy)ethyl]amino]benzaldehyde (**3**)

Anhydrous DMF (10 mL) was placed in a flask and was cooled in ice bath. Then 4.86 mL (50 mmol) phosphorus oxychloride was added dropwise with stirring. After the solution was stirred at 0 °C for 30 min, 10 g *N*,*N*-di(2-acetyloxy)ethyl] amino]benzene (40 mmol) in 6 mL DMF was added dropwise into the red solution to react for 1 h, then heated at 90 °C for 2 h. The reaction mixture was cooled to 0 °C, and neutralized to pH ≈ 7 by dropwise addition of saturated sodium acetate solution. The mixture was extracted with ethyl acetate. The extracts were washed with water, dried with magnesium sulfate, and then concentrated by rotary evaporation. The residue was purified by an aluminium oxide column using ethyl acetate/petroleum ether mixture (1:1 v/v) as eluent to give a pale yellow solid. Yield: 90%. FT-IR (KBr), n (cm^{-1}): 1737, 1660 (C═O), 1593, 1521 (−Ar), 1240 (C−O). ^1H NMR (300 MHz, $CDCl_3$), δ (ppm): 2.01 (6H, s, CH_3), 3.73 (4H, t, $J = 6.2$ Hz, CH_2CH_2OAc), 4.22 (4H, t, $J = 6.2$ Hz, CH_2CH_2OAc), 6.78 (2H, d, $J = 8.9$ Hz, 2- and 6-H), 7.71 (2H, d, 3- and 5-H), 9.79 (1H, s, C*H*O).

2.2.4. 4-[N,N-Di[2-hydroxyethyl]amino]benzaldehyde (**4**)

2.93 g (10 mmol) 4-[*N*,*N*-di[2-(acetyloxy)ethyl]amino]benzaldehyde was added to 25 mL ethanol and 25 mL (10%) sodium hydroxide water solution. After the reaction mixture had been stirred for 7 h at room temperature, the product was neutralized with dilute hydrochloric acid. Then the solvent was removed under reduced pressure and the residue was extracted with ethyl acetate. The extracts were washed with water, dried with magnesium sulfate, and then concentrated to give a yellow solid of 1.74 g (80%). FT-IR (KBr), n (cm^{-1}): 3379 (−OH), 2945 ($-CH_2$), 1657 (C═O), 1597, 1526 (−Ar), 1173 (C−O). ^1H NMR (300 MHz, $CDCl_3$), δ (ppm): 3.66 (4H, t, $J = 6.2$ Hz, CH_2CH_2OH), 3.90 (6H, t, CH_2CH_2OH), 6.70 (2H, d, $J = 8.9$ Hz, 2- and 6-H), 7.7 (2H, d, 3- and 5-H), 9.65 (1H, s, C*H*O).

2.2.5. 4-Bromobenzyl bromide (**5**)

1.19 g (7 mmol) 4-bromotoluene was dissolved in 15 mL CCl_4 under stirring. To the transparent solution was added 1.25 g (7 mmol) *N*-bromosuccinimide and 17 mg benzoyl peroxide. Then the reaction was heated at 80 °C for 2 h under nitrogen. After the mixture was cooled to room temperature, the white precipitate was filtered and the filtrate was concentrated. The crude product was recrystallized from ethanol-ethyl acetate twice to give white crystals in 61% yield. FT-IR (KBr), n (cm^{-1}): 2974 ($-CH_2$), 708, 590 (C−Br). ^1H NMR (300 MHz, $CDCl_3$), δ (ppm): 4.21 (2H, s, CH_2Br), 7.32 (2H, d, $J = 13.1$ Hz, 2- and 6-H), 7.49 (2H, d, 3- and 5-H).

2.2.6. 4-Bromobenzyl(triphenyl)phosphonium bromide (**6**)

To a 250 mL flask with a stirrer, 25 g (0.10 mol) 4-bromobenzyl bromide, 30 g (0.11 mol) triphenylphosphine and 200 mL toluene were added. The reaction mixture was refluxed for 3 h and then cooled to room temperature and filtered. The resulting white solid was filtered and then recrystallized from ethanol to give colorless crystals in 75% yield. FT-IR (KBr), n (cm^{-1}): 1435, 1484 (Ar−P). ^1H NMR (300 MHz, $CDCl_3$), δ (ppm): 5.41 (2H, s, CH_2), 7.12–7.83 (19H, m, Ar).

2.2.7. 4-Bromo-4′-(N,N-di-2-hydroxyethyl)stilbene (**7a**)

To a 250 mL three-necked flask with a dropping funnel, a nitrogen input tube and an adapter with a stopcock, 2.93 g (10 mmol) 4-[*N*,*N*-di[2-(acetyloxy)ethyl]amino]benzaldehyde, 5.38 g (10.5 mmol) 4-bromobenzyl(triphenyl)phosphonium bromide and 100 mL THF were added under a nitrogen atmosphere. The reaction mixture was cooled to 0 °C in an ice bath, 60 mmol potassium *tert*-butoxide–*tert*-butyl alcohol solution was added to the dropping funnel and was dropped into

the flask at 0 °C over 1 h. After the reaction mixture had been stirred for 2 h at 0 °C, the ice bath was removed and the mixture stirred at room temperature overnight. The product was neutralized with dilute hydrochloric acid and filtered. The resulting solid was purified by column chromatography using ethyl acetate/petroleum ether mixture (1:2 v/v) as eluent to give 1.63 g pale yellow solid in 45% yield. FT-IR (KBr), n (cm^{-1}): 3338 (−OH), 2945 ($-CH_2$), 1607 (−Ar). ^1H NMR (300 MHz, DMSO-d_6), δ (ppm): 3.44 (4H, t, $J = 6.1$ Hz, CH_2 CH_2OH), 3.54 (4H, t, CH_2CH_2OH), 4.71 (2H, s, OH), 6.69 (2H, d, $J = 8.7$ Hz, 1-H), 6.91 (1H, d, $J = 16.4$ Hz, 10-H), 7.12 (1H, d, 9-H), 7.41 (2H, d, $J = 8.6$ Hz, 4-H), 7.49 (2H, d, 3-H), 7.49 (2H, d, 2-H) (the serial number of hydrogen atom of benzene ring is given in Scheme 1).

2.2.8. N-((4-N,N-Dihydroxyethylamino)benzylidene)-4-bromoaniline (**7b**)

1.05 g (5 mmol) 4-[*N*,*N*-di[2-hydroxyethyl]amino]benzaldehyde and 0.86 g (5 mmol) 4-bromoaniline were dissolved in 50 mL benzene and 0.5 mL acetic acid glacial. The reaction mixture was refluxed for 10 h and water formed by the reaction was removed azeotropically by with Dean−Stark trap. Then the solvent was removed under reduced pressure and the residue was re-crystallized in ethanol to give dark yellow crystals of 1.25 g (69%). FT-IR (KBr), n (cm^{-1}): 3358 (−OH), 2877 ($-CH_2$), 1600, 1522 (−Ar). ^1H NMR (300 MHz, DMSO-d_6), δ (ppm): 3.50 (4H, t, $J = 5.7$ Hz, CH_2CH_2OH), 3.58 (4H, t, CH_2CH_2OH), 4.82 (2H, s, OH), 6.78 (2H, d, $J = 8.8$ Hz, 1-H), 7.14 (2H, d, $J = 8.6$ Hz, 4-H), 7.53 (2H, d, 3-H), 7.69 (2H, d, 2-H), 8.41 (1H, s, CH═N).

2.2.9. 4-Bromo-4′-(N,N-di-2-hydroxyethyl)azobenzene (**7c**)

4-Bromoaniline (3.44 g, 20 mmol) was dissolved in an ice-water solution of sodium nitrite (1.36 g, 20 mmol). After cooling to 0 °C, the solution was added to conc. hydrochloric acid (8 mL) and stirred for 30 min. Then the mixture was added dropwise to 400 mL aqueous buffer solution of acetic acid−sodium acetate (pH ≈ 6) containing 3.81 g *N*,*N*-di-(2-hydroxyethyl)aniline (21 mmol) and stirred for 2 h at 0−5 °C. The resulting precipitate was filtered and rinsed with water twice. The crude product was recrystallized from ethanol twice to give yellow crystals in 83% yield (6.04 g). FT-IR (KBr), n (cm^{-1}): 3280 (−OH), 2945, 2882 ($-CH_2$), 1597 (−Ar). ^1H NMR (300 MHz, DMSO-d_6), δ (ppm): 3.55 (4H, t, $J = 5.5$ Hz, CH_2CH_2OH), 3.60 (4H, t, CH_2CH_2OH), 4.84 (1H, s, OH), 6.86 (2H, d, $J = 9.1$ Hz, 1-H), 7.70 (2H, d, $J = 8.9$ Hz, 4-H), 7.76 (2H, d, 3-H), 7.85 (2H, d, 2-H).

2.2.10. 4′-(N,N-dihydroxyethylamino),4-(pyridine-4-vinyl) stilbene (**8a**)

Under nitrogen 1.81 g (5 mmol) 4-bromo-4′-(*N*,*N*-di-2-hydroxyethyl)stilbene, 11.2 mg $Pd(OAc)_2$ (0.05 mmol), 26.2 mg (0.10 mmol) PPh_3, 0.07 mL (7.5 mmol) vinylpyridine were dissolved in 50 mL DMF. The resultant mixture was refluxed for 24 h. After cooling to room temperature, the reaction solution was added to water to precipitate the product. The precipitate was washed three times using ethanol to give yellow-green powder in 80% yield. $T_m = 283$–285 °C. FT-IR (KBr), n (cm^{-1}): 3372 (−OH), 2883 ($-CH_2$), 1588, 1520 (−Ar). ^1H NMR (300 MHz, DMSO-d_6), δ (ppm): 3.52 (4H, t, $J = 6.0$ Hz, CH_2CH_2OH), 3.55 (4H, t, CH_2CH_2OH), 4.70 (2H, s, OH), 6.70 (2H, d, $J = 8.6$ Hz, 1-H), 7.02 (1H, d, $J = 16.3$ Hz, 7-H), 7.18 (1H, d, $J = 16.4$ Hz, 10-H), 7.21 (1H, d, 9-H), 7.40 (2H, d, $J = 8.5$ Hz, 4-H), 7.41 (1H, s, 8-H), 7.55 (2H, d, 3-H), 7.57 (2H, d, 2-H), 7.62 (2H, d, $J = 8.1$ Hz, 5-H), 8.53 (2H, d, 6-H). Elem. Anal. Calcd for $C_{25}H_{26}N_2O_2$: C, 77.72; H, 6.74; N, 7.25. Found: C, 77.65; H, 6.73; N, 7.21.

2.2.11. N-((4-N,N-dihydroxyethylamino)benzylidene)-4-(pyridine-4-vinyl)aniline (**8b**)

This was prepared as above from *N*-((4-*N*,*N*-dihydroxyethylamino)benzylidene)-4-bromoaniline. The precipitate was washed three times using ethanol to give brown-yellow solid powder in 81% yield. $T_m = 289$–291 °C. FT-IR (KBr), n (cm^{-1}): 3416 (−OH), 2927 ($-CH_2$), 1604, 1576, 1391 (−Ar). ^1H NMR (300 MHz, DMSO-d_6), δ (ppm): 3.52 (4H, t, $J = 6.0$ Hz, CH_2CH_2OH), 3.59 (4H, t, CH_2CH_2OH), 4.78 (2H, s, OH), 6.82 (2H, d, $J = 8.7$ Hz, 1-H), 7.20 (1H, d, $J = 16.3$ Hz, 7-H), 7.25 (2H, d, $J = 8.3$ Hz, 4-H), 7.54 (1H, d, 8-H), 7.56 (2H, d, 3-H), 7.68 (2H, d, 2-H), 7.73 (2H, d, $J = 8.5$ Hz, 5-H), 8.47 (1H, s, CH═N), 8.55 (2H, d, 6-H). Anal. Calcd for $C_{24}H_{25}N_3O_2$: C, 74.42; H, 6.46; N, 10.85. Found: C, 74.41; H, 6.56; N, 10.88.

2.2.12. 4′-(N,N-dihydroxyethylamino),4-(pyridine-4-vinyl) azobenzene (**8c**)

This was prepared as above from 4-bromo-4′-(*N*,*N*-di-2-hydroxyethyl)azobenzene. The precipitate was washed for three times using ethanol to give red-brown powder in 80% yield. $T_m = 297$–299 °C. FT-IR (KBr), n (cm^{-1}): 3483 (−OH), 2943 ($-CH_2$), 1598, 1512 (−Ar). ^1H NMR (300 MHz, DMSO-d_6), δ (ppm): 3.56 (4H, t, $J = 6.0$ Hz, CH_2CH_2OH), 3.60 (4H, t, CH_2CH_2OH), 4.88 (2H, s, OH), 6.86 (2H, d, $J = 8.9$ Hz, 1-H), 7.37 (1H, d, $J = 16.3$ Hz, 7-H), 7.64 (2H, d, $J = 7.7$ Hz, 4-H), 7.72 (1H, d, 8-H), 7.77 (2H, d, 3-H), 7.80 (2H, s, 2-H), 7.82 (2H, d, $J = 8.1$ Hz, 5-H), 8.58 (2H, d, 6-H). Elem. Anal. Calcd for $C_{23}H_{24}N_4O_2$: C, 71.13; H, 6.19; N, 14.43. Found: C, 71.44; H, 6.25; N, 14.45.

3. Results and discussion

3.1. Synthesis

We designed the molecular structure of three novel organic optical materials with different delocalized π-electron conjugation bridge. The reaction routes for their syntheses are shown in Scheme 1. Synthesis of compounds **1**–**7** is based on the method reported by us [18–20]. The Heck reaction of compounds **7a**, **7b**, and **7c** with 4-vinylpyridine using $Pd(OAc)_2/PPh_3$ as catalyst give long conjugated organic optical compounds **8a**, **8b**, and **8c** in high yield. We characterized all the intermediates and objective compound molecules using standard spectroscopic methods and obtained satisfactory analysis of data corresponding to their molecular structure.

3.2. The ground-state absorption spectra

The UV spectra of objective compounds **8a**, **8b**, and **8c** in THF are shown in Fig. 1. Compound **8a** exhibits absorption peak at 410 nm associated with corresponding the π−π* transition of the long conjugated chromophore. The maximum UV spectral absorption of compound **8b** shifts from 410 nm of **8a** to 394 nm when the conjugation bridge varies from C═C to C═N double bond, while compound **8c** with N═N double bond as conjugation bridge shows the UV absorption peak at 468 nm, hinting that the π-electron conjugation bridge has significant effect on their ground state electron absorption spectra of molecules and **8c** molecule possesses larger π-electron delocalized degree than **8a** and **8b**. Simultaneously, we found in Fig. 1 that **8a** and **8b** have almost no absorption at 532 nm while **8c** shows a weak absorption at 532 nm.

3.3. Nonlinear optical properties

The nonlinear absorption coefficients of **8a**, **8b** and **8c** were measured by using Z-scan technique. In our experiment, the samples were moved along the direction of laser beam around the focus ($z = 0$) forward or backward. The transmittance was recorded by a power meter with an aperture in the far field of lens as the function of sample position. The results of Z-scan with an aperture showed that **8a** and **8c** have strong nonlinear absorption (Figs. 2 and 3) while **8b** has only weak nonlinear absorption (Fig. 4).

In theory, the normalized transmittance for the open aperture can be written as [17,21]:

$$T(z, s = 1) = \sum_{m=0}^{\infty} \frac{[-q_0(z)]^m}{(m+1)^{3/2}}, \quad \text{for } |q_0| < 1 \tag{1}$$

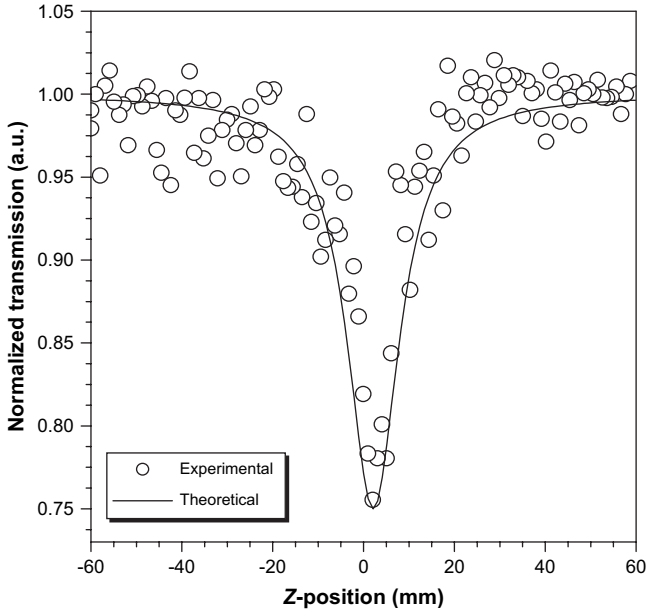

Fig. 2. Open Z-scan data of **8a**. Open circle: experimental data; solid line: theoretical curve.

where $q_0(z) = \alpha_2 I_0(t) L_{\text{eff}} / \left(1 + z^2/z_0^2\right)$, α_2 is the nonlinear absorption coefficient, $I_0(t)$ is the intensity of laser beam at focus ($z = 0$), $L_{\text{eff}} = [1 - \exp(-\alpha_0 L)]/\alpha_0$ is the effective thickness with α_0 the linear absorption coefficient and L the sample thickness, z_0 is the diffraction length of the beam, and z is the sample position. Thus, the nonlinear absorption coefficients of **8a**, **8b** and **8c** can be determined by fitting the experimental data using Eq. (1) to be 1.41×10^{-11}, 0.89×10^{-11}, 2.24×10^{-11} m/W, respectively.

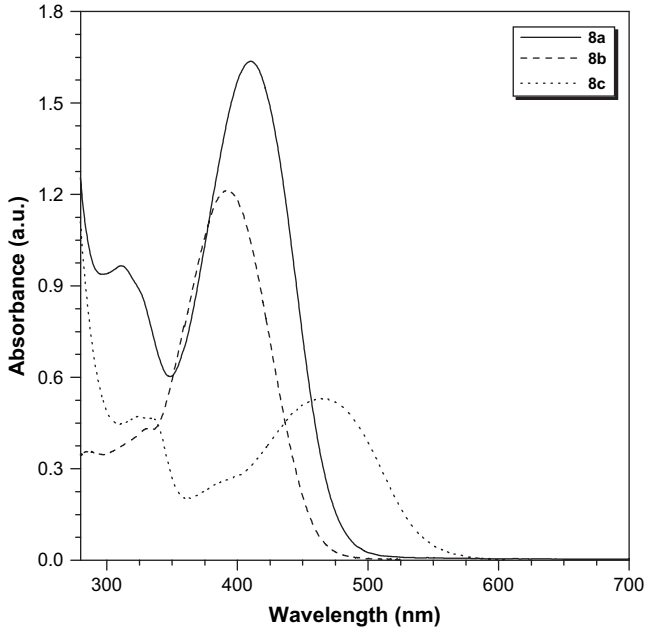

Fig. 1. UV−vis spectra of **8a** (solid line), **8b** (dash line) and **8c** (dot line) in THF solution (concentration: 0.01 mg/mL in THF).

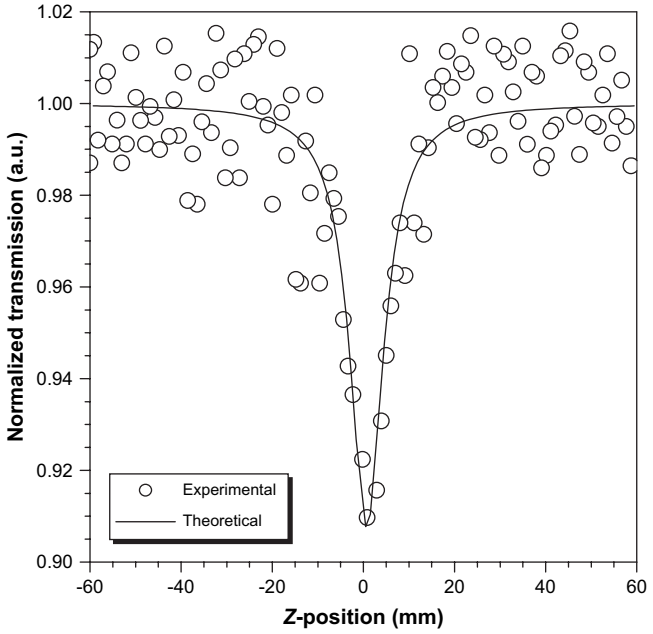

Fig. 3. Open Z-scan data of **8c**. Open circle: experimental data; solid line: theoretical curve.

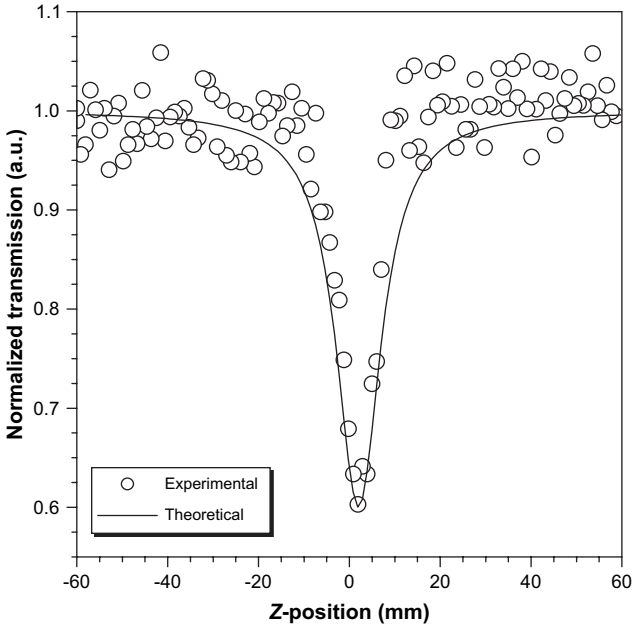

Fig. 4. Open Z-scan data of **8b**. Open circle: experimental data; solid line: theoretical curve.

The imaginary third-order nonlinear susceptibilities Im $\chi^{(3)}$ can be calculated by the following equation:

$$\text{Im}\,\chi^{(3)}\,(\text{esu}) = 9\times 10^{8}\,\frac{\varepsilon_0 n_0^2 c^2 \alpha_2}{4\pi\omega} \tag{2}$$

where ε_0 is the permittivity of vacuum, c is the speed of light, and n_0 is the refractive index of the medium and $\omega = 2\pi c/\lambda$. Therefore, the results can be calculated and listed in Table 1. From Table 1, it can be seen that Im $\chi^{(3)}$ is 4.0×10^{-12}, 6.3×10^{-12} and 9.1×10^{-12} esu for **8a**, **8b** and **8c**, respectively. These nonlinear absorption coefficients are larger than that of [4-(4′-cyanoazophenylyl)oxy]-1-hexanol reported by Xu et al. [22]. The large nonlinear absorption coefficient can be attributed to the long π-electron delocalized effect of **8a**, **8b** and **8c**. Simultaneously, it can also be found that the nonlinear susceptibilities of **8a** and **8c** are larger than that of **8b** and the compound **8c** with N=N double bond as conjugated bridge shows the largest third-order nonlinearity. Comparing the structures of **8a**, **8c** and **8b**, it can be seen that they are only different from the conjugated bridge between benzene rings linking with the 4-vinylpyridine. From the crystal structures of stilbene, *N*-benzilidene aniline and azobenzene [23–26], it is well known that stilbene and azobenzene mainly adopt the plan structure in the molecules while *N*-benzilidene aniline is usually considered to possess the non-planar structure in the molecules due to the distort of the two adjacent benzene rings along with the single bond. Therefore, the low nonlinear susceptibilities of **8b** molecules could be attributed to its nonplanarity. The results are consistent with that of their electron absorption spectra.

Table 1
The optical properties of **8a**, **8b** and **8c**

Compound	Nonlinear optical values[a]		Optical limiting values	
	α_2 (m/W)	Im $\chi^{(3)}$ (esu)	T_{NL}[b]	σ_{eff}/σ_0
8a	1.41×10^{-11}	6.3×10^{-12}	0.42	3.9
8b	0.89×10^{-11}	4.0×10^{-12}	–	–
8c	2.24×10^{-11}	9.1×10^{-12}	0.49	3.2

[a] Measured by Z-scan technique with an 8 ns Nd:YAG laser system at 1 Hz repetition rate and 532 nm wavelength.
[b] Nonlinear transmittance at saturated output fluence.

3.4. Optical limiting properties

Fig. 5 shows the optical limiting performance of **8a**, **8b** and **8c** at the same linear transmittance ($T = 80\%$). From Fig. 5, it can be seen that, at very low incident fluence, the output fluence of **8a**, **8b** and **8c** solutions with 80% transmittance linearly increases with the incident fluence obeying the Beer–Lambert law. However, at high incident fluence, the transmittance of the solution decreased (the incident fluence starting to deviate from linear transmittance is defined as limiting threshold), and a nonlinear relationship is observed between the output and input fluence, and with a further increase in the incident fluence, the transmitted fluence reaches a plateau (limiting amplitude), showing the well optical limiting property. Simultaneously, the optical limiting properties are significantly affected by the π-electron conjugation bridge structure of molecules. The saturated absorption of compound **8a** happens in the incident fluence of 1.65 J/cm^2, while the saturated absorption of compound **8c** in the incident fluence of 1.85 J/cm^2. The **8a** shows the limiting threshold at 0.149 J/cm^2 and limiting amplitude at 0.69 J/cm^2 while the limiting thresholds for **8b** and **8c** are at 0.26 J/cm^2 and 0.25 J/cm^2, respectively, and the limiting amplitude for **8c** at

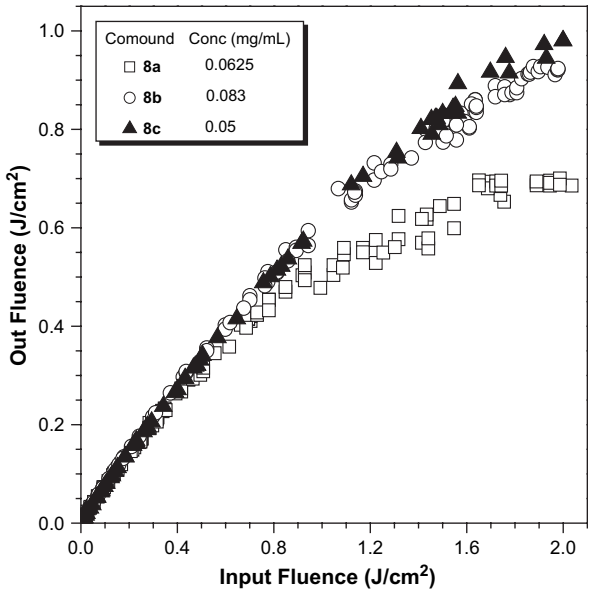

Fig. 5. Optical responses to 8 ns, 1 Hz pulses of 532 nm laser light of **8a** (open squares), **8b** (close triangles), and **8c** (open circles) solution with a linear transmission of 80%.

0.91 J/cm^2. It is seen that **8a** shows better optical limiting property than **8b** and **8c**.

The optical limiting mechanisms of organic compounds are often based on two-photon absorption (TPA) or reverse saturable absorption (RSA). Generally, TPA-based optical-limiting effect can be yielded in principle under the laser irradiation of picosecond or shorter pulses. RSA is achieved on a nanosecond or longer time scale, rather than a picosecond time scale, owing to the different excited-state lifetimes involved in a multilevel energy process [15]. In the work, the molecules are excited by the laser with 8 ns pulse width at 532 nm wavelength and the transmittance of all these compounds' solution decreases with the increase of the incident fluence. Therefore, we can consider that the optical limiting properties of **8a**, **8b** and **8c** may arise from RSA.

The optical limiting property of molecules for RSA mechanism depends on the ratio of the excited state absorption cross-section (σ_{ex}) to the ground state absorption cross-section (σ_g) of molecules, which was defined as $\sigma_{ex}/\sigma_0 = \ln T_{sat}/\ln T_0$. T_{sat} is the transmittance at saturated output fluence [27]. It is seen in Fig. 1 that **8c** shows strong ground state electron absorption at 532 nm wavelength, hinting that the **8c** molecule has large ground state absorption cross-section, while **8a** displays weak ground state electron absorption at 532 nm wavelength, showing that **8a** may possess small ground state absorption cross-section for the laser with 532 nm wavelength to result in the larger ratio of σ_{eff}/σ_0 than **8c**. We can estimate the σ_{ex}/σ_0 based on saturated transmittance of compounds **8a** and **8c** solutions. As shown in Table 1, the corresponding value of σ_{eff}/σ_0 for **8a** is calculated to be 3.88, while σ_{ex}/σ_0 for **8c** is 3.19. It may be why **8a** shows better optical limiting property than **8c** although **8c** displays better nonlinear optical property than **8a**.

4. Conclusions

The three novel organic optical materials with different π-electron conjugation bridge structure are synthesized in satisfactory yield by Heck reaction. Their structures are characterized by standard spectroscopic method. Their optical limiting and nonlinear optical properties are investigated by an 8 ns Nd:YAG laser system at 532 nm wavelength. The results show that the optical limiting and nonlinear optical performance are affected by π-electron conjugation bridge structure. The compound with N═N double bond as conjugation bridge shows the best nonlinear optical property and the compound with C═C double bond as conjugation bridge displays the best optical limiting property, which is attributed to the larger σ_{ex}/σ_0.

Acknowledgements

This research was financially supported by the National Natural Science Fund of China (Grant Nos. 90206014 and 50472038), the Program for New Century Excellent Talents in University of China (NCET-04-0588), the Excellent Youth Fund of Anhui Province (Grant No. 04044060), and the Award for High Level Intellectuals (Grant No. 2004Z027) from Anhui Province.

References

[1] Tutt LW, Kost A. Nature 1992;356:225.
[2] Tutt LW, Boggess TF. Prog Quantum Electron 1993;17:299.
[3] Aderson HL, Martin SJ, Bradeley DC. Angew Chem Int Ed Engl 1994;33:655.
[4] Spanglar CW. J Mater Chem 1999;9:2013.
[5] Wang X, Liu CL, Gong QH, Huang YY, Huang CH. Opt Commun 2001;197:83.
[6] Chen Y, Song YL, Qu SL, Wang DY. Opt Mater 2001;18:219.
[7] Liu HW, Chen CF, Xi F, Wang P, Zhang S, Wu PJ, et al. J Nonlinear Opt Phys Chem 2001;4:423.
[8] Kiran PP, Srinivas NKMN, Reddy DR, Maiya BG, Dharmadhikari A, Sandhu AS, et al. Opt Commun 2002;202:347.
[9] Frutos EMG, O'Flaberty SM, Maya EM, Torre GDL, Blau W, Vazquez P, et al. J Mater Chem 2003;13:749.
[10] Sun WF, Byeon CC, Mckerns MM, Lawson CM, Gray GM, Wang DY. Appl Phys Lett 1998;73:1167.
[11] Wang P, Ming H, Xie JP, Zhang WJ, Gao XM, Xu Z, et al. Opt Commun 2001;192:387.
[12] Qu SL, Song YL, Du CM, Wang YX, Gao YC, Liu ST, et al. Opt Commun 2001;196:317.
[13] Zhou GJ, Zhang S, Wu PJ, Ye C. Chem Phys Lett 2002;363:610.
[14] Sun WF, Wu ZX, Yang QZ, Wu LZ, Tung CH. Appl Phys Lett 2003;82:850.
[15] Sun WF, Bader MM, Carvalho T. Opt Commun 2003;215:185.
[16] Yin SC, Xu HY, Su XY, Gao YC, Song YL, Lam JWY, et al. Polymer 2005;46:10592.
[17] BaHae MS, Said AA, Wei TH, Hagan DJ, Stryland EWV. IEEE J Quantum Electron 1990;26:760.
[18] Yin SC, Xu HY, Shi WF, Gao YC, Song YL, Lam JWY, et al. Polymer 2005;46:7670.
[19] Yin SC, Xu HY, Fang M, Shi WF, Gao YC, Song YL. Macromol Chem Phys 2005;206:1549.
[20] Tong BY, Xu HY, Yu Q, Guang SY, Tang BZ. Chin J Synth Chem 2003;12:103.
[21] Zhang C, Song YL, Wang X, Kühn FE, Wang YX, Fun HK, et al. J Mater Chem 2002;12:239.
[22] Xu XS, Ming H, Wang P, Liang ZC, Zhang QJ. J Opt A Pure Appl Opt 2002;4:L5.
[23] Nakai H, Shiro M, Ezumi K, Sakata S, Kubota T. Acta Crystallogr Sect B Struct Sci 1976;32:1827.
[24] Nakai H, Ezumi K, Shiro M. Acta Crystallogr Sect B Struct Sci 1981;37:193.
[25] Morley JO. J Mol Struct 1995;340:45.
[26] Morley JO. J Chem Soc Perkin Trans 1995;2:731.
[27] Perry JW, Mansour K, Marder SR, Perry K, Alvarez D, Choog I. Opt Lett 1994;19:625.